Paleoceanography and Paleoclimatology

Supporting Information for

Modern, pre-industrial and past (last 25 ka) carbon isotopic ($\delta^{13}C$) variability in the surface waters of the southwest Pacific

Charles Maxson[1], Helen Bostock[2], Andrew Mackintosh[1], Sara Mikaloff-Fletcher[2], Nick McCave[3], Helen Neil[2]

[1] Antarctic Research Centre, Victoria University, Wellington, New Zealand
[2] National Institute of Water and Atmospheric Research, Wellington, New Zealand
[3] Department of Earth Sciences, University of Cambridge, England

Contents of this file

Supplementary data 1: Testing the Multiple Linear Regression with the surface water $\delta^{13}C_{DIC}$ data from transect TAN1302 between New Zealand and Antarctica (Bass et al., 2014)

Supplementary data 2 Table and text: Multiple Linear Regression for the 1990s World Ocean Circulation Experiment (WOCE) transects

Supplementary data 3: Age models for cores TAN0803-27, TAN1106-7 and TAN1106-11

Supplementary data 4: Cross correlation analyses of paleoclimate datasets

Additional Supporting Information (Files uploaded separately - txt file)

Table S1 – Stable isotopes of *Globigerina bulloides* from cores tops.

Table S2 - Stable isotopes of *Globigerina bulloides* from all the cores in this study (see Table 4 in main text).

Table S3 – Sea surface temperature (SST) data used to temperature correct the $\delta^{13}C_{G.bulloides}$ data from the different regions.

Supplementary data 1: Testing the Multiple Linear Regression with the surface water $\delta^{13}C_{DIC}$ data from transect TAN1302 between New Zealand and Antarctica (Bass et al., 2014)

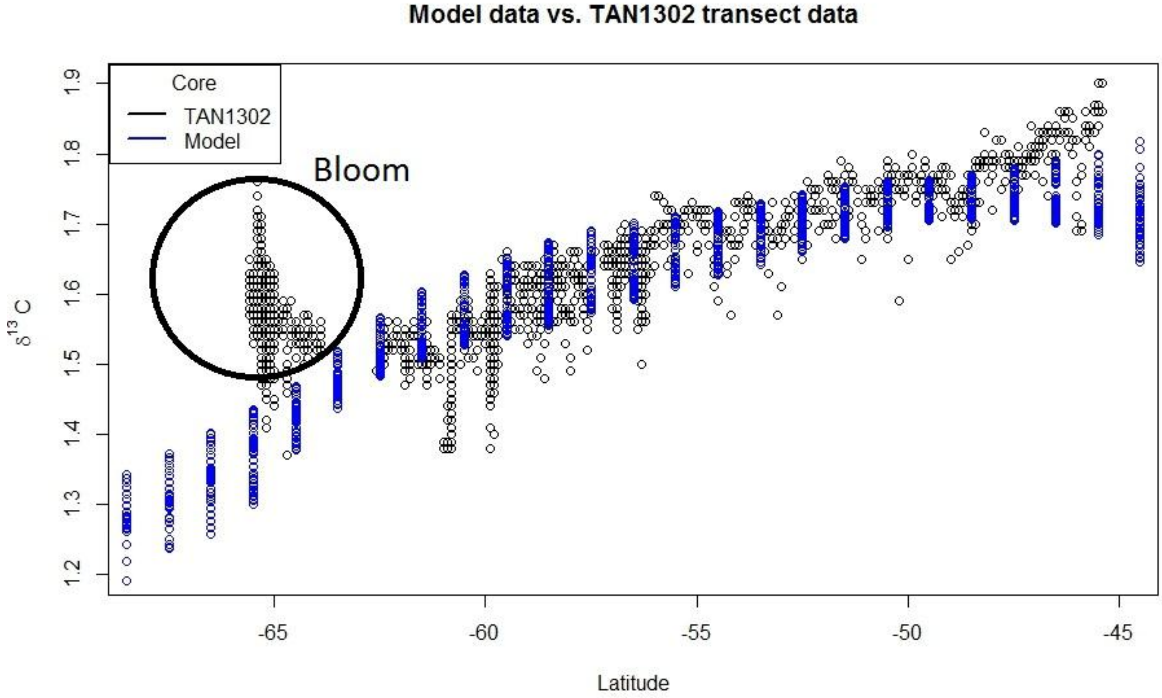

Supplementary Figure 1: Measured $\delta^{13}C_{DIC}$ surface water from voyage TAN1302 transect from New Zealand to Antarctica (Bass et al., 2014) compared to estimated $\delta^{13}C_{DIC}$ data from the MLR model. The northern and southern parts of the transect show $\delta^{13}C_{DIC}$ higher than the model predicts. The northern anomaly is associated with the STF east of New Zealand and the southern anomaly with a phytoplankton bloom in the surface waters of the Antarctic continental shelf. This highlights that the MLR is not able to replicate the $\delta^{13}C_{DIC}$ during high biological productivity.

Supplementary data 2: Multiple Linear Regression for the 1990s WOCE transects

Transect	**Dates**	**Ship**	**Principal Scientist**
SR3 (140-145°E)	22/08/1996-15/09/1996	RV Aurora Australis	B. Tilbrook
P06 (30-32.5°S)	02/05/1992-30/07/1992	RV Knorr	H. Bryden/M. McCartney/J. Toole
P15 (170-175°W)	05/01/1996-10/03/1996	RV Discoverer	R. Feely/J. Bullister
P16 (150°W)	06/10/1992-25/11/1992	RV Knorr	J. Reid
P18 (100°W)	26/01/1994-27/04/1994	RV Discoverer	G. Johnson/B. Taft
P19 (88°W)	22/02/1993-13/04/1994	RV Knorr	L. Talley

Supplementary Table: 1990s WOCE Transects used in the South Pacific (shown on Figure 1B)

The $\delta^{13}C_{DIC}$ measured on these transects are higher during the 1990s than in the 2000s and 2010s. Using the $\delta^{13}C_{DIC}$ data and hydrographic data from the 1990s WOCE voyages (Supp. Table 1) gives a slightly different MLR (equation 2).

$\delta^{13}C_{DIC}$ = 5.321 – (0.00305*AOU) + (0.159*θ) + (0.701*σ_θ) – (0.693*Salinity) **[2]**

R^2= 0.75, RMSE = 0.21 and sd = 0.43

The residuals (Model versus Observed) are shown in supplementary figure 2. There is a wider range of residuals than for the 2000s and 2010s data in the main text, but a similar pattern with higher residuals in the surface waters ±0.5‰, likely due to the biological productivity is not completely captured by the MLR estimates. Seasonal maps of the surface $\delta^{13}C_{DIC}$ for the southwest Pacific are shown in supplementary figure 3. These show a subtle seasonal surface $\delta^{13}C_{DIC}$ signal (likely an underestimate due to the residuals in the surface waters) with elevated values during the Austral spring and summer.

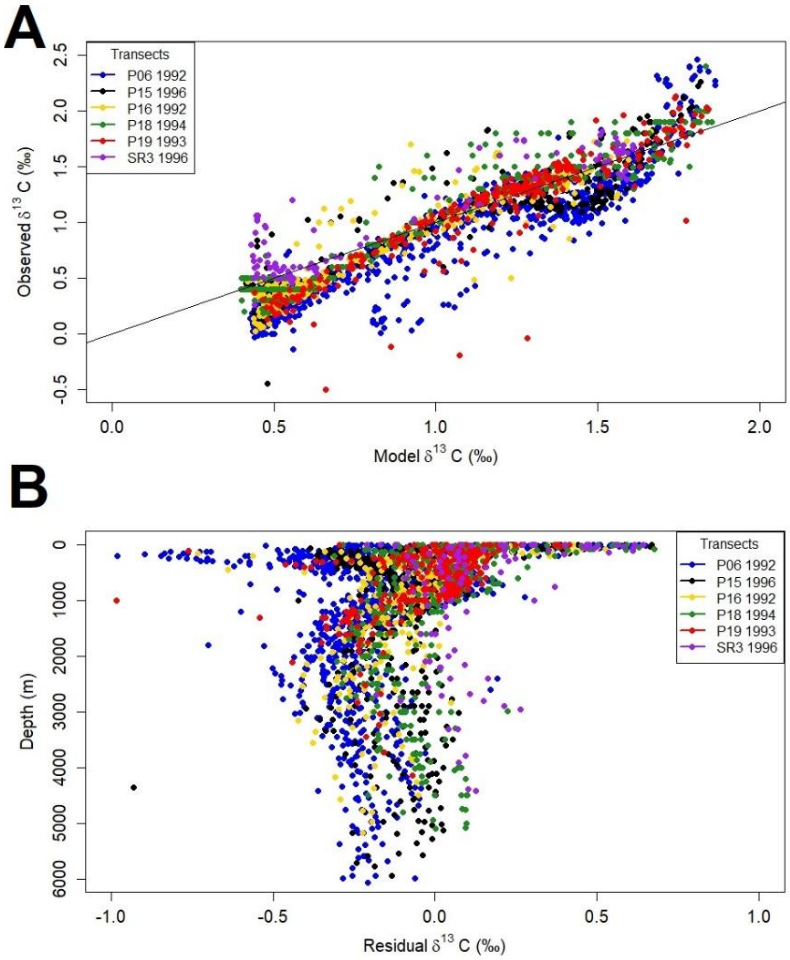

Supplementary Figure 2: A) Model versus observed $\delta^{13}C_{DIC}$ for 1990s transects and B) residuals (model versus observed) versus water depth.

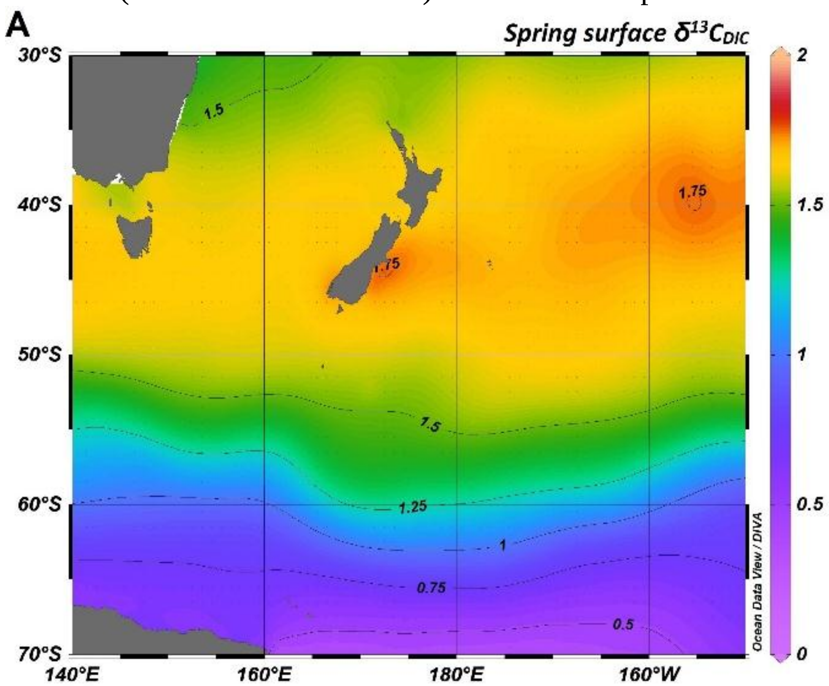

Supplementary Figure 3: $\delta^{13}C_{DIC}$ in the 1990s for Austral spring

Supplementary data 3: Age models for cores TAN0803-27, TAN1106-7 and TAN1106-11

Age models for 4 additional cores were developed using oxygen stable isotopes from the planktic foraminifera *Globigerina bulloides*, and radiocarbon ages. Radiocarbon analyses were undertaken on mixed planktic foraminifera and calibrated using a reservoir age ΔR -42 ± 39 (Rafter et al., 1972), using the MARINE13 calibration curve (Reimer et al., 2013), using the CALIB 7.1 program (Stuiver et al., 2018; http://calib.org/).

Core	Depth (cm)	Radiocarbon age	Calibrated age (2 sigma range) years BP	Median age (error) years BP	Reference
TAN1106-7	0	5455 ± 35	5727-5992	5877	This study
	40	10070 ± 60	10894-11253	11111	
	110	16260 ± 80	18932-19448	19171	
TAN1106-11	0	1570 ± 60	997-1297	1170	This study
	60	11030 ± 70	12445-12753	12606	
	120	13690 ± 60	15794-16251	16031	
TAN1106-15	75	4684 ±29	4827-5135	4961	This study (Prebble et al., 2017)
	100	5903 ± 28	6265-6466	6356	
	125	6869 ± 32	7310-7520	7423	
	170	8460 ± 36	8990-9274	9126	
	200	10065±39	10944-11230	11113	
TAN0803-27	0	2990 ± 35	2711-2929	2804	This study
	25	8210 ± 50	8595-8971	8786	
	50	11632 ± 65	12958-13325	13162	
	55	12665 ± 50	14033-14670	14263	

The oxygen stable isotope data and age models for these cores are available in the supplementary data.

Supplementary data 4: Cross correlation analyses of paleoclimate datasets

A cross correlation analysis was used to determine if there were any strong statistical relationships between the Monte Carlo simulation average temperature corrected $\delta^{13}C_{G.\ bulloides}$ records from each of the regions studied in this paper and other local and global paleo-climatic datasets for the last 25 ka. To do this all datasets were averaged into 1ka timeslices with two 500-year resolution points at 21.5 and 18.5ka. The points at 18.5 and 21.5ka record significant changes in one or more latitudinal zones that would not have been resolved with the 1000-year intervals, and thus were added. The raw data and 1ka averaged data are also shown in Figure 8.

	BoP	NCR	SCR	SolN	SolS	$\delta^{13}C_{atm}$	$\delta^{13}C_{LCDW}$	atmCO_2	$\delta^{13}C_{AAIW}$
BoP	1.00								
NCR	0.23	1.00							r>0.9
SCR	0.69	-0.13	1.00						r>0.8
SolN	0.61	0.10	0.91	1.00					r>0.7
SolS	0.51	-0.10	0.88	0.92	1.00				
$\delta^{13}C_{atm}$	0.59	0.43	0.39	0.57	0.41	1.00			
$\delta^{13}C_{LCDW}$	0.60	-0.30	0.91	0.75	0.80	0.24	1.00		
atmCO_2	0.58	-0.21	0.96	0.84	0.84	0.20	0.93	1.00	
$\delta^{13}C_{AAIW}$	0.13	-0.62	0.59	0.40	0.47	-0.05	0.72	0.73	1.00

Supplementary Table: Cross correlation analyses for the last 25 ka between the Monte Carlo simulation averaged (temperature corrected) $\delta^{13}C_{G.bulloides}$ data for the 5 different regions; BoP – Bay of Plenty, NCR – North Chatham Rise, SCR – South Chatham Rise, SolN – Solander Trough, North , SolS – Solander Trough, South. These are compared with paleoclimatic data; EPICA ice core $\delta^{13}C_{atm}$ (Eggleston et al., 2016); benthic foraminifera $\delta^{13}C_{LCDW}$ of *Cibicidoides wuellerstorfi* from LCDW south Tasman Sea (GC34) (Moy et al., 2006); atmospheric CO_2 levels from Antarctic ice core EDC – EPICA Dome C (Eggleston et al., 2016); and benthic foraminifera $\delta^{13}C_{AAIW}$ of *Cibicidoides wuellerstorfi* from AAIW from the flank of the Challenger Plateau west of New Zealand (SO136-3) (Ronge et al., 2015). Strong correlations (r>0.9) are highlighted in orange, good correlations (r>0.8) in yellow and weaker correlations (r>0.7) in light green.

The results suggest that there are no strong correlations between the northern regions BoP and NCR and any other region or paleoclimatic record. The southern regions SCR, SolN and SolS are strongly correlated (r=0.88 to 0.92) and show weak to strong correlations with the benthic foraminifera $\delta^{13}C_{LCDW}$ of *Cibicidoides wuellerstorfi* from the LCDW (Moy et al., 2006) and atmospheric CO_2 concentrations (Eggleston et al., 2016). Correlations between the southern regions and the AAIW $\delta^{13}C_{AAIW}$ of *Cibicidoides wuellerstorfi* (Ronge et al., 2015) and atmospheric $\delta^{13}C_{atm}$ from EPICA ice cores (Eggleston et al., 2016) are very weak (r=0.39-0.59).

References

Bass, A. M., Munksgaard, N. C., O'Grady, D., Williams, M. J., Bostock, H. C., Rintoul, S. R., & Bird, M. I. (2014). Continuous shipboard measurements of oceanic $\delta^{18}O$, δD and $\delta^{13}C_{DIC}$ along a transect from New Zealand to Antarctica using cavity ring-down isotope spectrometry. *Journal of Marine Systems, 137*, 21-27.

Eggleston, S., Schmitt, J., Bereiter, B., Schneider, R., & Fischer, H. (2016). Evolution of the stable carbon isotope composition of atmospheric CO_2 over the last glacial cycle. *Paleoceanography, 31*(3), 434-452.

Moy, A. D., Howard, W. R., & Gagan, M. K. (2006). Late Quaternary palaeoceanography of the circumpolar deep water from the South Tasman Rise. *Journal of Quaternary Science, 21*(7), 763-777.

Rafter, T.A., Jansen, H.S., Lockerbie, L., & Trotter, M.M. (1972). New Zealand reference standards. In: Rafter, T.A., Grant-Taylor, T., eds., Proceedings of the 8th International conference on 14C dating. Wellington. Royal Society of New Zealand, 2, H29-H79.

Reimer, P.J., Bard, E., Bayliss, A., Beck, J.W., Blackwell, P.G., Bronk Ramsey, C., Buck, C.E., Cheng, H., Edwards, R.L., Friedrich, M., Grootes, P.M., Guilderson, T.P., Haflidason, H., Hajdas, I., Hatte, C., Heaton, T.J., Hogg, A.G., Hughen, K.A., Kaiser, K.F., Kromer, B., Manning, S.W., Niu, M., Reimer, R.W., Richards, D.A., Scott, E.M, Southon, J.R., Turney, C.S.M., & van der Plicht, J. (2013). IntCal13 and MARINE13 radiocarbon calibration curves 0-50,000 years calBP. Radiocarbon 55, doi:10.2458/azu_ js_rc.55.16947.

Ronge, T. A., Steph, S., Tiedemann, R., Prange, M., Merkel, U., Nürnberg, D., & Kuhn, G. (2015). Pushing the boundaries: Glacial/interglacial variability of intermediate and deep waters in the southwest Pacific over the last 350,000 years. *Paleoceanography, 30*(2), 23-38.

Stuiver, M., Reimer, P.J., Reimer, R.W., 2018. CALIB 7.1 at http://calib.org